Quantum phase properties of the field in a lossless micromaser cavity

Tseresodnom Gantsog*
Max-Planck-Institut für Quantenoptik, Hans-Kopfermann-Strasse 1, D–85748 Garching, Germany

Ryszard Tanaś
Nonlinear Optics Division, Institute of Physics, Adam Mickiewicz University, 60-780 Poznań, Poland
(Received 16 May 1995)

Phase properties of the micromaser field are studied for different initial states of the cavity field and the atom. It is shown that a multipeak phase structure develops when the cavity field is initially in a coherent state and the atoms enter the cavity in their excited state, which eventually leads to the randomization of the phase. If initially the field is thermal and the atoms entering the cavity are polarized, the steady state with a considerably well defined phase is reached, which asymptotically can be one of the cotangent states or some mixed state depending on the atom-cavity interaction time. An interesting effect of switching between the two- and three-peak phase structure caused by each subsequent atom passing the cavity has been found.

PACS number(s): 42.50.Dv, 42.52.+x

I. INTRODUCTION

One of the marvelous experimental and theoretical systems for the study of truly quantum aspects of the interaction between radiation and matter is the one-atom maser, or micromaser [1–16]. A micromaser consists of a microwave cavity and a stream of excited atoms which drive the field inside the cavity. The beam is sufficiently sparse so that at most one atom at a time is present inside the cavity. The photon statistics of a micromaser shows interesting quantum effects including sub-Poissonian photon statistics [1,3,4] and collapse and revival of Rabi oscillations [5]. Even a number state can be generated using a cavity with a high enough quality factor and with no thermal photons [6]. Both conditions can be fulfilled when the superconducting cavity is operated at very low temperatures. In this case even more interesting features may show up, such as trapping states of the cavity [3,7]. Moreover, the micromaser allows us to prepare and measure the off-diagonal elements of the field density matrix [8]. The spectrum [9] and the phase diffusion coefficient [10–12] of the micromaser field, which involve the off-diagonal elements of the field density matrix, have been calculated, and a method of inferring them from the properties of the emerging atomic beam has been proposed. The possibility of generating a coherent state of the micromaser field has also been predicted [13]. One of the very intriguing features of the micromaser is the possibility of obtaining pure states of the field, so-called tangent and cotangent states [14], if the initial conditions are properly chosen. Phase properties and squeezing of the cotangent states have been studied by Meystre *et al.* [15].

In this paper, we consider the problem of quantum phase fluctuations of the field generated in the lossless micromaser cavity. In our discussion we use the Pegg-Barnett Hermitian phase formalism [17]. The phase probability distribution for different initial atomic and field states is calculated and its evolution illustrated graphically. We have found that the phase distribution function exhibits a number of interesting features. In particular, if the micromaser starts from the coherent field and is pumped by excited atoms the phase distribution function develops $N+1$ separate peaks as N atoms have passed through the cavity, suggesting the appearance of the superposition states. In fact, the sequence of more and more peaks that appear in the phase distribution for an increasing number of injected atoms leads to the randomization of the phase, i.e., to making the phase distribution more and more uniform.

On the other hand, if the maser cavity starts with thermal field and is driven by polarized atoms, the field in the cavity that initially had no preferred phase acquires some phase from the atoms, and a phase peak develops during the evolution. We show that the phase properties of the cavity field evolve to a steady state as the number of injected atoms increases, but character of this state depends strongly on the atomic interaction time. The existence of the trapping states has an impact on the phase properties of the micromaser field and, despite the fact that thermal field is defined on the whole Fock space, there are intervals of interaction times for which field asymptotically evolves to a pure state, which is an appropriate cotangent state, but there are also intervals of interaction time for which the resulting state is a mixed state.

An interesting effect appears when the cavity field is initially in a coherent state and the cavity is pumped by the polarized atoms. In this case two different phase structures, one with two phase peaks and another one with three peaks, develop. Each subsequent atom traversing the cavity switches the cavity field between the two structures. If the number of atoms that passes the cavity is odd, the two phase peaks are observed, and for an even number of atoms three peaks appear. The shape of the two phase distributions does not depend on the number of atoms that passes the cavity but on the parity of this number.

The paper is organized as follows. In Sec. II, we derive the exact recursion relation for the field reduced density ma-

*Permanent address: Department of Theoretical Physics, National University of Mongolia, 210646 Ulaanbaatar, Mongolia.

trix. In Sec. III, we shortly review the Pegg-Barnett phase formalism which we use in the further parts of the paper. In Sec. IV, we study the phase properties of the micromaser field for different initial atomic and field states. Finally, Sec. V contains a conclusion.

II. QUANTUM EVOLUTION OF THE FIELD STATE

The Hamiltonian describing the interaction of a single two-level atom with a quantized cavity field is given, in the dipole and rotating-wave approximations and in the interaction picture, by [5]

$$H=\hbar g(a|a\rangle\langle b|+a^{\dagger}|b\rangle\langle a|). \tag{1}$$

Here the operator $|i\rangle\langle j|$ $(i\neq j)$ describes the transition from level j to level i, a and $a^{\dagger}$ are the photon annihilation and creation operators of the cavity mode, and g is the atom-cavity mode coupling constant, which we assume to be real. The transition between the atomic upper level a and the lower level b is assumed to be resonant with the cavity mode. This simplified model is usually referred to as the Jaynes-Cummings model.

The dynamics associated with the Jaynes-Cummings model are exactly soluble [5]. By using the relation $|i\rangle\langle j||k\rangle\langle l|=|i\rangle\langle l|\delta_{kj}$ we can easily show that

$$\begin{aligned}(H/\hbar)^{2k}&=g^{2k}[(aa^{\dagger})^{k}|a\rangle\langle a|+(a^{\dagger}a)^{k}|b\rangle\langle b|],\\ (H/\hbar)^{2k+1}&=g^{2k+1}[(aa^{\dagger})^{k}a|a\rangle\langle b|+(a^{\dagger}a)^{k}a^{\dagger}|b\rangle\langle a|],\end{aligned} \tag{2}$$

where k $(k\geqslant 0)$ is an integer number. Hence, the time-evolution operator $U(t)$ of the atom-field system can be expressed in the form [5,18]

$$\begin{aligned}U(t)&\equiv\exp(-iHt/\hbar)\\ &=\cos(gt\sqrt{a^{\dagger}a+1})|a\rangle\langle a|+\cos gt\sqrt{a^{\dagger}a})|b\rangle\langle b|\\ &\quad -i\frac{\sin(gt\sqrt{a^{\dagger}a+1})}{\sqrt{a^{\dagger}a+1}}a|a\rangle\langle b|\\ &\quad -i\frac{\sin(gt\sqrt{a^{\dagger}a})}{\sqrt{a^{\dagger}a}}a^{\dagger}|b\rangle\langle a|.\end{aligned} \tag{3}$$

The matrix elements of this operator are

$$\begin{aligned}\langle a;n|U(t)|a;n'\rangle&=\cos(\Omega_n t)\,\delta_{nn'},\\ \langle b;n|U(t)|b;n'\rangle&=\cos(\Omega_{n-1}t)\,\delta_{nn'},\\ \langle a;n|U(t)|b;n'\rangle&=-i\,\sin(\Omega_n t)\,\delta_{nn'-1},\\ \langle b;n|U(t)|a;n'\rangle&=-i\,\sin(\Omega_{n-1}t)\,\delta_{nn'+1}.\end{aligned} \tag{4}$$

where we have used the notation $\Omega_n=g\sqrt{n+1}$.

Let the atoms be initially prepared in a coherent superposition of their states,

$$\begin{aligned}\rho_{\mathrm{A}}&=\rho_{aa}|a\rangle\langle a|+\rho_{bb}|b\rangle\langle b|+\rho_{ab}|a\rangle\langle b|+\rho_{ba}|b\rangle\langle a|\\ &=\sum_{i,j=a,b}\rho_{ij}|i\rangle\langle j|,\end{aligned} \tag{5}$$

where

$$\begin{aligned}&\rho_{ii}\geqslant 0,\quad \rho_{aa}+\rho_{bb}=1,\quad \rho_{ab}=\rho_{ba}^{*},\\ &|\rho_{ab}|=|\rho_{ba}|\leqslant\sqrt{\rho_{aa}\rho_{bb}},\end{aligned} \tag{6}$$

and be injected into a lossless microwave cavity at such a low rate that at most one atom at a time is present inside the cavity. We assume that the time of the interaction of each atom with the cavity field is much shorter than the lifetime of all the atomic levels. Then the atomic spontaneous decay processes to other levels or other modes can be ignored while an atom is inside the cavity, which means that the joint evolution of the cavity field and atoms is unitary. For simplicity, we suppose that the injected atoms have the same velocity and, therefore, interact with the cavity field for the same time. We denote this interaction time by τ.

Moreover, since there is a free evolution of the field density matrix in the time between the subsequent atoms enter the cavity, i.e. the matrix elements $\rho(n,n')$ acquire an extra phase factor $\exp(i(n-n')\omega\delta t)$, where ω is the cavity resonance frequency and δt is the time between the arrivals of subsequent atoms, we assume here that the time δt is chosen in such a way that ωt is equal to a multiple of 2π. In this case the extra phase factor due to the free evolution is unity and can be discarded. Otherwise we should take it into account in the overall density matrix evolution. If the atoms were arriving at random times they would meet the cavity field with random phases, and the cavity field phase which is associated with the nondiagonal elements of the field density matrix would necessarily become random (only diagonal elements would survive). This assumption is a very serious restriction to the model considered here. It means that atoms should be injected into the cavity in a well controllable way, which, of course, will not be easy to achieve in a real experimental situation.

Assuming that this is possible, the field density matrix ρ evolves according to

$$\rho_{N+1}=\mathrm{Tr}_{\mathrm{A}}[U(\tau)\rho_{\mathrm{A}}\otimes\rho_N U^{\dagger}(\tau)]. \tag{7}$$

Here ρ_N is the density matrix of the field after N atoms have passed through the cavity and Tr_{A} stands for trace over the atomic variables. In writing Eq. (7) we have assumed that the state of the atom is not measured as it exits the cavity. The number of injected atoms N is considered as a scaled evolution time of the system.

By using Eq. (7) together with the expressions (4) and (5), we can easily get for the field density-matrix elements the recursion relation

$$\rho_{N+1}(n,n')=\rho_{aa}[\cos(\Omega_n\tau)\cos(\Omega_{n'}\tau)\rho_N(n,n')+\sin(\Omega_{n-1}\tau)\sin(\Omega_{n'-1}\tau)\rho_N(n-1,n'-1)]$$
$$+\rho_{bb}[\cos(\Omega_{n-1}\tau)\cos(\Omega_{n'-1}\tau)\rho_N(n,n')+\sin(\Omega_n\tau)\sin(\Omega_{n'}\tau)\rho_N(n+1,n'+1)]$$
$$+i\rho_{ab}[\cos(\Omega_n\tau)\sin(\Omega_{n'}\tau)\rho_N(n,n'+1)-\sin(\Omega_{n-1}\tau)\cos(\Omega_{n'-1}\tau)\rho_N(n-1,n')]$$
$$-i\rho_{ba}[\sin(\Omega_n\tau)\cos(\Omega_{n'}\tau)\rho_N(n+1,n')-\cos(\Omega_{n-1}\tau)\sin(\Omega_{n'-1}\tau)\rho_N(n,n'-1)]. \quad (8)$$

Given the initial state of the cavity field $\rho(0)\equiv\rho_{N=0}=\rho_0$, the recursion relation (8) allows us to obtain the field density matrix $\rho_N(n,n')$ for any N.

It is clear from Eq. (8) that the coupling between the diagonal matrix elements $\rho_{N+1}(n,n)$ and the off-diagonal elements $\rho_N(n,n\pm1)=\rho_N^*(n\pm1,n)$ occurs only when the atomic coherence $\rho_{ab}=\rho_{ba}^*$ is present. If the micromaser starts from the vacuum or from a thermal field, and is pumped by unpolarized atoms (i.e., $\rho_{ab}=\rho_{ba}=0$), then the off-diagonal elements of the field density matrix always remain equal to zero, and consequently, the field phase is always random. However, atoms prepared in a coherent superposition of their states via microwave field before entering the micromaser cavity create nonvanishing off-diagonal elements; that is, they create a preferred field phase [8].

In Sec. IV we study the phase properties of the field state defined by Eq. (8), for different initial atomic and field states.

III. REVIEW OF THE PEGG-BARNETT HERMITIAN PHASE FORMALISM

To describe quantum phase properties of the field, generated in the ideal microwave cavity, we apply the Hermitian phase formalism introduced by Pegg and Barnett [17]. This formalism is based on introducing a finite $(s+1)$-dimensional space Ψ spanned by the number states $|0\rangle$, $|1\rangle$, ..., $|s\rangle$, for a given mode of the field. The Hermitian phase operator operates on this finite space and, after all necessary expectation values have been calculated in Ψ, the value of s is allowed to tend to infinity. A complete orthonormal basis of $(s+1)$ states is defined on Ψ as

$$|\theta_m\rangle\equiv\frac{1}{\sqrt{s+1}}\sum_{n=0}^{s}\exp(in\theta_m)|n\rangle, \quad (9)$$

where

$$\theta_m\equiv\theta_0+\frac{2\pi m}{s+1}, \quad m=0,1,\ldots,s. \quad (10)$$

The value of θ_0 is arbitrary and defines a particular basis set of $(s+1)$ mutually orthogonal phase states. The Hermitian phase operator is defined as

$$\hat{\phi}_\theta\equiv\sum_{m=0}^{s}\theta_m|\theta_m\rangle\langle\theta_m|, \quad (11)$$

where the subscript θ indicates the dependence on the choice of θ_0. The phase states (9) are eigenstates of the phase operator (11) with the eigenvalues θ_m restricted to lie within a phase window between θ_0 and $\theta_0+2\pi$.

The expectation value of the kth power of the phase operator (11) in a state described by the density operator ρ is given by

$$\langle\hat{\phi}_\theta^k\rangle=\mathrm{Tr}\{\rho\hat{\phi}_\theta^k\}=\sum_{m=0}^{s}\theta_m^k\langle\theta_m|\rho|\theta_m\rangle, \quad (12)$$

where $\langle\theta_m|\rho|\theta_m\rangle$ gives a probability of being found in the phase state $|\theta_m\rangle$. The density of phase states is $(s+1)/2\pi$, so in the continuum limit as s tends to infinity, we can write Eq. (12) as

$$\langle\hat{\phi}_\theta^k\rangle=\int_{\theta_0}^{\theta_0+2\pi}\theta^kP(\theta)d\theta, \quad (13)$$

where the continuum phase distribution $P(\theta)$ is introduced by

$$P(\theta)=\lim_{s\to\infty}\frac{s+1}{2\pi}\langle\theta_m|\rho|\theta_m\rangle$$
$$=\frac{1}{2\pi}\sum_{n,n'=0}^{\infty}\rho(n,n')\exp[-i(n-n')\theta], \quad (14)$$

with θ_m being replaced by the continuous phase variable θ. Here $\rho(n,n')$ are the matrix elements of the density operator in the number state basis. Once the phase distribution function $P(\theta)$ is known, all the quantum-mechanical phase expectation values can be calculated with this function in a classical-like manner by integrating over θ. The choice of θ_0 defines a particular window of phase values.

Of particular interest in description of the phase properties of the field is the phase variance that can be calculated according to the formula

$$(\Delta\hat{\phi})^2=\int\theta^2P(\theta)d\theta-\left[\int\theta P(\theta)d\theta\right]^2. \quad (15)$$

The phase probability distribution illustrates the phase structure of the field mode while the variance provides a good understanding of the evolution of the field phase fluctuations.

Since the number and phase are conjugate quantities, they obey the uncertainty relation [17]

$$\Delta n\Delta\phi\geq\frac{1}{2}|\langle[\hat{n},\hat{\phi}]\rangle|. \quad (16)$$

The number-phase commutator appearing on the right-hand side of Eq. (16) can be easily evaluated, for any physical state, from the relation [17]

$$\langle[\hat{n},\hat{\phi}]\rangle=i[1-2\pi P(\theta_0)]. \quad (17)$$

So, both sides of the uncertainty relation (16) can be calculated independently for a given state of the field, and the uncertainty relation itself can be tested for finding, for example, the minimum uncertainty states. We use the field characteristics defined above to study quantum phase properties of a lossless micromaser.

IV. PHASE PROPERTIES OF THE MICROMASER FIELD FOR DIFFERENT INITIAL ATOMIC AND FIELD STATES

In this section we study phase properties of the micromaser field using the Pegg-Barnett phase formalism. Since the phase behavior of the micromaser field strongly depends on the state of the field initially existing in the cavity as well as on whether the atoms are injected into the cavity in their excited state or in a superposition of their excited and ground states, we consider separately the case of incoherent and coherent pumping.

A. The case of no injected atomic coherence

Here we consider the case when $\rho_{ab}=\rho_{ba}=0$, that is, no atomic coherence is injected into the cavity. We assume that atoms are injected into the cavity in their excited state, i.e., $\rho_{aa}=1$ and $\rho_{bb}=0$. In this case, the evolution of the field density matrix is governed by the equation

$$\rho_N(n,n')=\cos(g\tau\sqrt{n+1})\cos(g\tau\sqrt{n'+1})\rho_{N-1}(n,n') + \sin(g\tau\sqrt{n})\sin(g\tau\sqrt{n'})\rho_{N-1}(n-1,n'-1). \tag{18}$$

According to Eqs. (14) and (18) the phase probability distribution of the micromaser field after N atoms have traversed the cavity is given by

$$P_N(\theta)=\frac{1}{2\pi}\sum_{n,n'=0}^{\infty}\rho_N(n,n')\exp[-i(n-n')\theta] = \frac{1}{2\pi}\sum_{n,n'=0}^{\infty}\rho_{N-1}(n,n')\cos[g\tau(\sqrt{n+1} - \sqrt{n'+1})]\exp[-i(n-n')\theta]. \tag{19}$$

For $N=1$, Eq. (19) reproduces the corresponding result obtained for the Jaynes-Cummings model [19]. From Eqs. (18) and (19), it is obvious that matrix elements of the density operator $\rho_N(n,n')$ and, consequently, the phase probability distribution $P_N(\theta)$ are very strongly dependent on the value of $g\tau$. This parameter can be varied experimentally by changing the velocity of the atomic beam.

One property of the micromaser field is obvious from the form of Eqs. (8) and (19). If the cavity field is initially in a photon number state or in a thermal state, then the nondiagonal elements of the field density operator are always equal to zero, and we have flat phase distribution $P_N(\theta)=1/(2\pi)$, that is, the phase of the field is completely random. So, if the field had no preferred phase initially and the cavity is pumped incoherently, i.e., by the atoms being in their excited state, the phase will always remain random. This is obvious, since there is no initial coherence in the field and the driving atoms do not also carry any phase information.

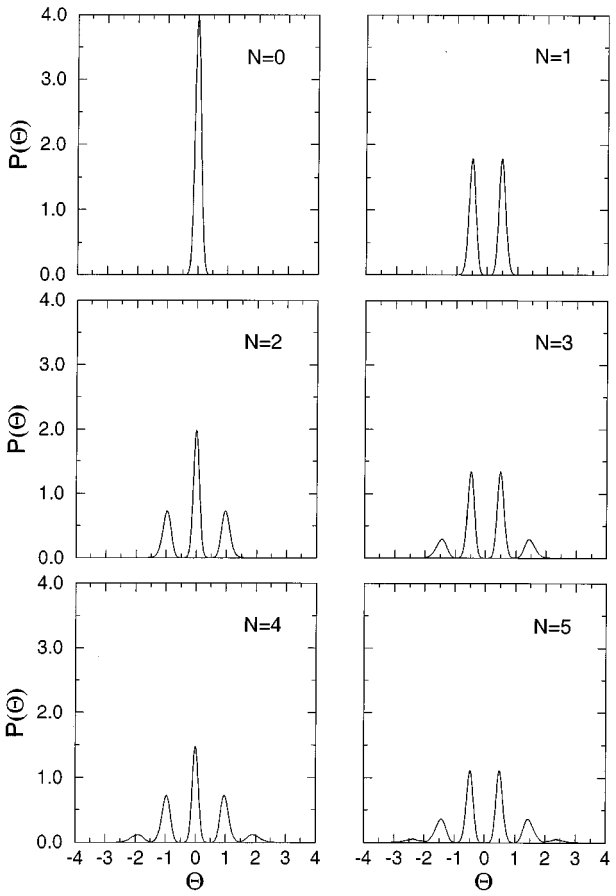

FIG. 1. Phase distribution $P(\theta)$ for initially coherent field with the mean number of photons $\bar{n}=25$, for $g\tau=5$ and various values of the number of injected atoms N.

The situation is quite different, however, if the field in the micromaser cavity has been prepared, before injecting the excited atoms, in a state which exhibits a phase peak, i.e., its phase is not random. Such a state can be, for example, a coherent state which can be prepared in the micromaser cavity under special conditions [13] or one of the cotangent states [14]. Now, we suppose that the cavity field is initially in the coherent state $\rho_0=|\alpha\rangle\langle\alpha|$ with $\alpha=\sqrt{\bar{n}}$, where $\bar{n}$ is the mean number of photons in the coherent state. We numerically calculate the development of the phase probability distribution $P_N(\theta)$ from Eq. (19) for $\bar{n}=25$, $g\tau=5$, and for various values of N using the recursion relation (18). The results are illustrated in Fig. 1, where the function $P_N(\theta)$ is plotted as a function of θ after $N=0$, 1, 2, 3, 4, and 5 atoms have passed through the cavity.

As seen from Fig. 1, the phase probability distribution of the initial coherent field ($N=0$) splits into $N+1$ separate peaks with different heights. The splitting occurs, however, differently depending on whether the number of injected atoms N is even or odd. For an even N the peaks appear at the phase angles $\theta=0,\pm1,\pm2,\ldots$ rad and the phase of initial coherent state is partially preserved, while for an odd N it is completely lost and the peaks appear at $\theta=\pm\frac{1}{2}$, $\pm\frac{3}{2}$, $\pm\frac{5}{2}$, . . . rad. The splitting of the distribution $P_N(\theta)$ sug-

gests that the state of the micromaser field evolves during the evolution into a superposition of distinguishable states with definite mean phases. With increasing N, the number of peaks in the distribution $P_N(\theta)$ increases, and as a result the distribution becomes more and more uniform, which means the randomization of the phase. The route to the random-phase distribution, however, goes through a sequence of an increasing numbers of peaks.

In the limit of large mean photon numbers ($\bar{n}\gg N$) an analytical treatment of the phase distribution function is available. To show this, we first make a Taylor expansion of $\sqrt{n+1}$ in Eq. (19) around the $\sqrt{\bar{n}+1}$ to get

$$\sqrt{n+1}=\sqrt{\bar{n}+1}+\frac{n-\bar{n}}{2(\bar{n}+1)^{1/2}}-\frac{(n-\bar{n})^2}{8(\bar{n}+1)^{3/2}}+\cdots. \tag{20}$$

Now we assume that for $\bar{n}\gg N$ the size of the region in which the field density matrix is essentially different from zero is not a large quantity compared to $\sqrt{\bar{n}}$. This condition is certainly satisfied for short times $g\tau$ and a small number of atoms $N\ll\bar{n}$. Then, for the number states that contribute significantly to the sum (19), one expects $(n-\bar{n})^2$ to be of order of, or smaller than, $\bar{n}$; hence for $g\tau\ll 2\pi\sqrt{\bar{n}}$, the third term on the right-hand side of Eq. (20) and all higher-order terms may be ignored to yield

$$g\tau(\sqrt{n+1}-\sqrt{n'+1})\simeq\frac{g\tau}{2\sqrt{\bar{n}}}(n-n'). \tag{21}$$

Then the distribution (19) becomes

$$P_N(\theta)\simeq\frac{1}{2\pi}\sum_{n,n'}\rho_0(n,n')\left\{\cos\left[\frac{g\tau}{2\sqrt{\bar{n}}}(n-n')\right]\right\}^N \times\exp[-i(n-n')\theta]. \tag{22}$$

Finally, using $\cos x=(e^{ix}+e^{-ix})/2$, we obtain from Eq. (22) the expression

$$\begin{aligned}P_N(\theta)&\simeq\frac{1}{2^N}\sum_{l=0}^{N}\binom{N}{l}\frac{1}{2\pi}\sum_{n,n'=0}^{\infty}\rho_0(n,n')\\&\quad\times\exp\left[-i(n-n')\left(\theta-\frac{N-2l}{2\sqrt{\bar{n}}}g\tau\right)\right]\\&=\sum_{l=0}^{N}a_l^N P_0(\theta-\varphi_l),\end{aligned} \tag{23}$$

where

$$P_0(\theta-\varphi_l)=\frac{1}{2\pi}\sum_{n,n'=0}^{\infty}\rho_0(n,n')\exp[-i(n-n')(\theta-\varphi_l)] \tag{24}$$

is simply the phase probability distribution for a coherent field $|\alpha\exp(i\varphi_l)\rangle$ with the amplitude $\alpha=\sqrt{\bar{n}}$ and the phase $\varphi_l=(N-2l)g\tau/(2\sqrt{\bar{n}})$ $(l=0,1,2,\ldots,N)$, and

$$a_l^N=\frac{1}{2^N}\binom{N}{l},\quad\sum_{l=0}^{N}a_l^N=1 \tag{25}$$

is a weight factor. The expression (23) has a very simple structure: the phase distribution $P_N(\theta)$ is a superposition of $N+1$ phase distributions for coherent states $P_0(\theta-\varphi_l)$ having different weights a_l^N and different mean phases φ_l.

Further, for an even N Eq. (23) can be written in the explicit form

$$P_N(\theta)=a_{N/2}^N P_0(\theta)+\sum_{l=0}^{N/2-1}a_l^N[P_0(\theta-\varphi_l)+P_0(\theta+\varphi_l)]. \tag{26}$$

Similarly, for an odd N we have

$$P_N(\theta)=\sum_{l=0}^{(N-1)/2}a_l^N[P_0(\theta-\varphi_l)+P_0(\theta+\varphi_l)]. \tag{27}$$

Equations (23)–(27) make the behavior of the phase probability distribution quite transparent. The $N+1$ peaks appear symmetrically with respect to the origin $\theta=0$. For an even N the highest peak is located at $\theta=0$, and for an odd N there are two peaks of equal height symmetrically placed with respect to the origin. The height of the lth peak is $1/a_l^N$ times smaller than that of the initial coherent-state peak ($N=0$). For our choice of $g\tau=5$ and $\bar{n}=25$, we have for the mean phases the value $\varphi_l=N/2-l$, which can be either an integer (for an even N) or half an integer (for an odd N). These analytical results are in good agreement with the exact numerical calculations presented in Fig. 1.

Surprisingly, the same results have been obtained for a cooperative Dicke model [20]. Such similarity stems from the fact that the interaction of subsequently injected atoms with the cavity field is, in a sense, also a cooperative process [13,16]. In both the Dicke model and the micromaser model under consideration the atoms interact with one another only through the cavity field. The only difference between the two models is the way atoms interact with the cavity field. In the Dicke model all the atoms simultaneously interact with exactly the same field while, in contrast, in the micromaser case each atom interacts with the field that was prepared by the previous atoms traversing the cavity, which is generally different but carries the prints of the atoms that created it.

In Fig. 2 we plot the phase variance $(\Delta\phi)^2$ as a function of the number of injected atoms N for $\bar{n}=25$ and $g\tau=1$, 5, 10, and 15. Note that for our choice of the phase window the second term in Eq. (15), and consequently the mean phase, is always equal to zero. Due to the central peak at $\theta=0$ (see Fig. 1), the phase variance for an even N is always less than that for an odd N. Therefore the phase variance shows the odd-even oscillations (Fig. 2). As we see from Fig. 2, the oscillations appear to be more pronounced for $gt\sim gt_R/2=\pi\sqrt{\bar{n}}$. For $g\tau=g\tau_R/2$, due to mutual overlap of the peaks the phase distribution function has just two peaks, which appear at $\theta=\pm\pi/2$ for an odd N and at $\theta=0,\pm\pi$ for an even N. The phase variance for these two structures has quite distinct values. As the number of injected atoms increases the phase variance asymptotically approaches $\pi^2/3$ — the value for the uniformly distributed phase.

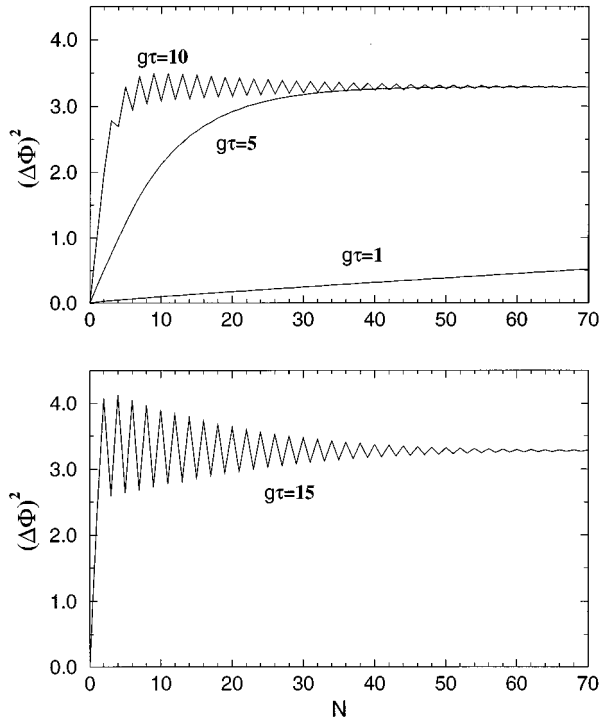

FIG. 2. Phase variance $(\Delta\phi)^2$ as a function of the number of injected atoms N, for initially coherent field with the mean number of photons $\bar{n}=25$, and for various values of $g\tau$.

The only assumption we used in our derivation of Eq. (22), or equivalently Eqs. (23)–(27), was the approximation (21), that is, the requirement that the initial field has a narrow photon number distribution. Therefore, similar behavior can also be expected for other states with a narrow photon number distribution. To illustrate this point we plot in Fig. 3 the phase probability distribution for the 1-cotangent state bound between the vacuum state $|0\rangle$ and the trapping state $|20\rangle$. This state can be prepared in a lossless micromaser cavity pumped by a stream of strongly polarized two-level atoms [14]. In our calculation for Fig. 3 we have chosen $g\tau=4$. As it is seen from Fig. 3, a multipeak phase structure also develops when the cavity field is in the 1-cotangent state and the atoms enter the cavity in their excited state. Similarly to the case of the coherent state, atoms injected in the excited state into the micromaser cavity containing the field with some phase structure cause degradation of this phase structure up to the complete randomization of the phase.

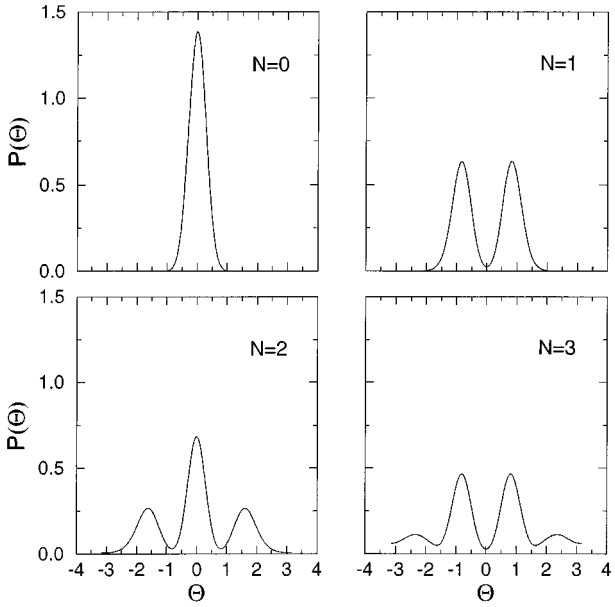

FIG. 3. Phase distribution $P(\theta)$ for initially 1-cotangent state bound between the vacuum $|0\rangle$ and the trapping state $|20\rangle$, for $g\tau=4$ and various values of the number of injected atoms N.

B. The case of injected atomic coherence

Now, we proceed to investigate the effect of the atomic coherence on the phase properties of the micromaser field. In this case, as we mentioned before, the atomic phase can be transferred to the cavity field, and we can expect a buildup of the phase structure even for the field that had no such structure initially. Let us assume that the atoms are injected into the cavity in a coherent superposition of the upper and lower states with $\rho_{ab}=\rho_{ba}^{*}=|\rho_{ab}|e^{i\varphi}$, where φ is the atomic initial phase and $|\rho_{ab}|=\sqrt{\rho_{aa}(1-\rho_{aa})}$. It is convenient to introduce the following definition for the density matrix:

$$\rho_N(n,n')=(-ie^{i\varphi})^{n-n'}\tilde{\rho}_N(n,n'). \tag{28}$$

Substituting this expression into Eq. (8), we can easily verify that $\tilde{\rho}_N(n,n')$ is a real and symmetric matrix [provided the initial matrix $\tilde{\rho}_0(n,n')$ is real] and does not depend on the atomic phase φ. The phase probability distribution can now be written as

$$P(\theta)=\frac{1}{2\pi}\sum_{n,n'=0}^{\infty}\tilde{\rho}_N(n,n')\exp[-i(n-n')\theta], \tag{29}$$

where we have chosen for the reference phase the value $\theta_0=\varphi-3\pi/2$. To choose the phase window to be symmetric with respect to the origin, we have chosen for the atomic phase the value $\varphi=\pi/2$.

Using Eqs. (29), (15), and (8)we have numerically calculated the phase variance for the cavity field assuming that initially it was in the thermal state. The results are presented in Fig. 4. It is seen that as the number of photons increases the phase variance approaches a steady-state value which depends on the value of $g\tau$, i.e., on the atom-field interaction time. We have assumed that atoms are strongly polarized with $\rho_{aa}=|\rho_{ab}|=0.5$. For small values of $g\tau$ ($g\tau<1$) it is evident from Fig. 4 that the micromaser field develops preferred phase and its phase variance drops to relatively small values as the number of atoms increases. In this case the atomic phase has been effectively transferred to the field. For greater values of $g\tau$ the phase variance becomes larger and the field phase is not very well defined. For still higher $g\tau$ (e.g., around $g\tau=4$) oscillations appear in the phase variance at the initial stage of the process, and it goes down to smaller values for a large number of atoms. The qualitatively different behavior of the phase variance for small and large values of $g\tau$ is quite obvious from the figure. For better understanding of the field evolution, we plot in Fig. 5 the mean number of photons and in Fig. 6 the normalized stan-

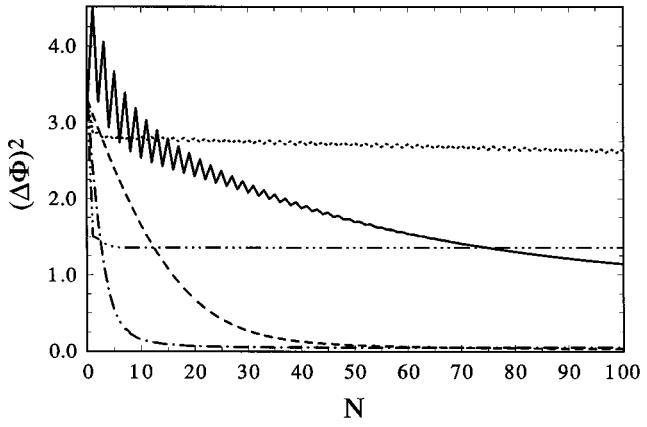

FIG. 4. Phase variance $(\Delta\phi)^2$ against the number of injected atoms N for various values of the scaled interaction time: $g\tau=0.1$ (dashed line), $g\tau=0.5$ (dot-dashed line), $g\tau=2$ (dot-dot-dashed line), $g\tau=3$ (dotted line), and $g\tau=4$ (solid line). The cavity field is initially in the thermal state with the mean number of photons $\bar{n}_b=0.1$ and is pumped by polarized atoms with $\rho_{aa}=\rho_{ab}=1/2$.

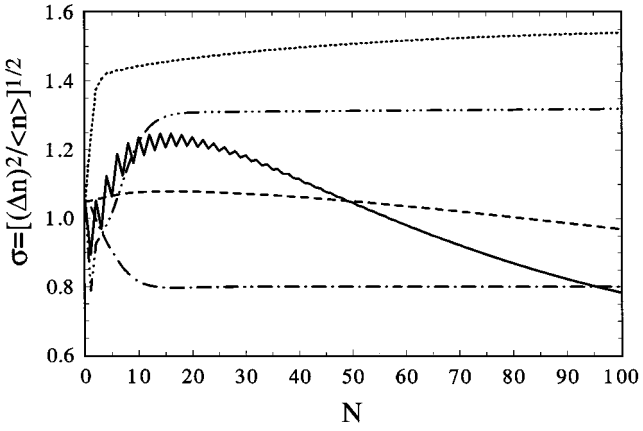

FIG. 6. Normalized standard deviation σ against the number of injected atoms N. The initial conditions, the parameters, and the meaning of the lines are the same as in Fig. 4.

dard deviation of the number of photons for the same values of the parameters as in Fig. 4. Again we can see the qualitative difference in behavior for the various intervals of τ. For small $g\tau$ the mean number of photons takes on considerable values and the photon statistics are sub-Poissonian. For $g\tau$ above unity the mean number of photons becomes small and its fluctuations bigger, and the statistics become super-Poissonian. For still higher value (around $g\tau=4$) the mean number of photons increases and the statistics become sub-Poissonian again.

To gain deeper insight into the physics behind these pictures we have calculated the states purity parameter defined as $\zeta=1-\mathrm{Tr}(\rho^2)$, which is plotted in Fig. 7. This parameter tends to zero if the field state tends to a pure state. From Fig. 7 we immediately see that for small values of $g\tau$ the purity parameter goes to zero as the number of atoms increases. This means that the field asymptotically goes to a pure state. We can identify these states as 1-cotangent states considered in [15] although the initial field was the thermal field which has no obvious truncation number. This can be explained by the fact that the thermal field photon distribution has its peak for the vacuum and decays as the number of photons increases, which means that for a sufficiently large number of photons the probability of finding a photon is so low that it can be treated practically as zero. For given $g\tau$ the upward trapping state $|M\rangle$ can be evaluated by $M+1=(\pi/g\tau)^2$ and, if this number is sufficiently large as to have a small probability of finding a photon in this state, this state can be treated as effectively truncating the photon distribution and the field state evolves to the corresponding 1-cotangent state. Phase properties of such states have been studied in [15].

If, however, $g\tau$ is bigger so the truncation number estimated in this way is so small that states above this number are essentially populated, or if the estimated truncation number is smaller than unity, the state of the field no longer evolves to one of the 1-cotangent states. For these intervals of the interaction time the field state becomes a mixed state, and its phase properties are substantially different. In this range of the interaction times the transfer of atomic phase to the field is not very effective and the field phase remains almost random with a rather flat phase distribution and a large phase variance. To make the qualitative difference of

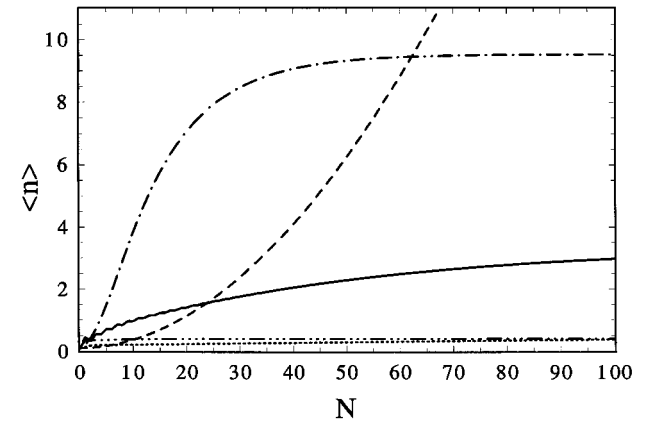

FIG. 5. Mean number of photons $\langle n\rangle$ against the number of injected atoms N. The initial conditions, the parameters, and the meaning of the lines are the same as in Fig. 4.

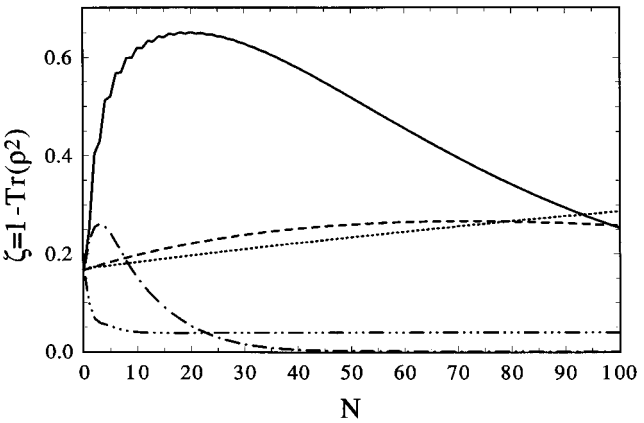

FIG. 7. Purity parameter ζ against the number of injected atoms N. The initial conditions, the parameters, and the meaning of the lines are the same as in Fig. 4.

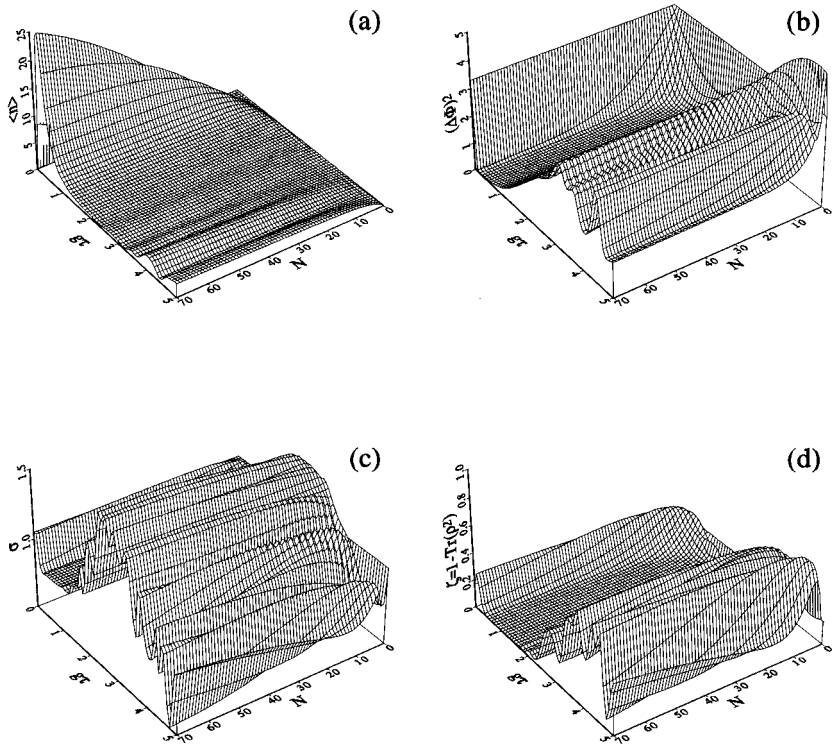

FIG. 8. Plots of (a) mean number of photons, (b) phase variance, (c) normalized standard deviation, and (d) purity parameter as functions of N and $g\tau$. The initial conditions and the parameters are the same as in Fig. 4.

the micromaser field properties for various regions of the $g\tau$ values more clear, we plot in Fig. 8 the three-dimensional pictures of the quantities discussed above, which show in a more spectacular way the differences in the micromaser field properties.

However, it is also seen from Fig. 8(d) that there are values of $g\tau>1$ for which the purity parameter drops almost to zero. This would suggest that even for bigger values of $g\tau$ the micromaser field can evolve close to a pure state, but this happens for a very narrow range of $g\tau$ values, and it is not easy to identify such states.

Knowing the phase variance and the photon number variance we can plot the number-phase uncertainty product which is presented in Fig. 9. The lower curve shows the lower bound to the uncertainty product given by the value of one-half of the modulus of the mean value of the number-phase commutator. It is seen from Fig. 9 that for small values of $g\tau$ actual uncertainty asymptotically approaches its lower bound. For those values of $g\tau$ for which the field evolves to a mixed state there is a gap between the actual uncertainty product and its lower bound.

In our discussion so far of the case when the atoms are injected to the micromaser cavity in a superposition of their states we have assumed that the cavity field is initially the thermal field with the mean number of photons equal to 0.1. We were looking at the possibility to build up some phase structure of the micromaser field that initially had no such structure. Now, let us assume that we have initially prepared the micromaser field in a state with a preferred phase, for example in a coherent state, and we ask what happens with such field when we drive the cavity with polarized atoms? In Fig. 10 we illustrate such situation: the initial field is in a coherent state with the mean number of photons equal to 25, and the atoms are injected in the superposition state with $\rho_{ab}=\sqrt{\rho_{aa}(1-\rho_{aa})}$. We plot the phase distribution $P(\theta)$ versus ρ_{aa} for the number of atoms that passed through the cavity equal to $N=2,\ 3,\ 50,\ 51$. The result is very interesting, because apart from the cases when atoms are in one of their stationary states ($\rho_{aa}=0,1$), the phase distribution exhibits two phase peaks for all odd numbers of atoms and three phase peaks for even numbers of atoms. Moreover, the shape of the distribution practically does not depend on the number of atoms injected to the cavity but depends on whether this number was odd or even. So each subsequent atom switches the phase distribution from a two-peak into a three-peak structure, and vice versa. We get the odd-even oscillation of the phase distribution, which is similar to the

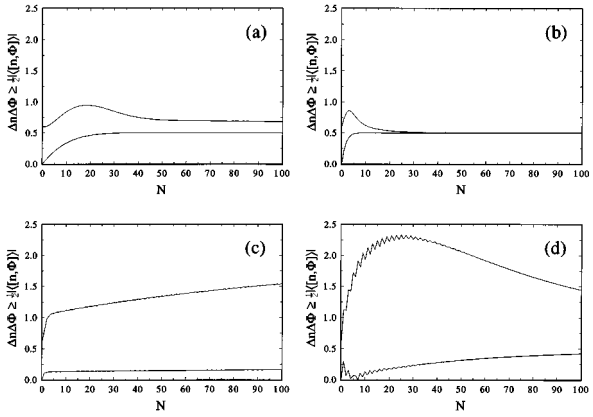

FIG. 9. Number-phase uncertainties as functions of N for various values of $g\tau$: (a) $g\tau=0.1$, (b) $g\tau=0.5$, (c) $g\tau=3$, and (d) $g\tau=4$. Upper and lower curves are the left- and right-hand sides of Eq. (16), respectively. The initial conditions and the other parameters are the same as in Fig. 4.

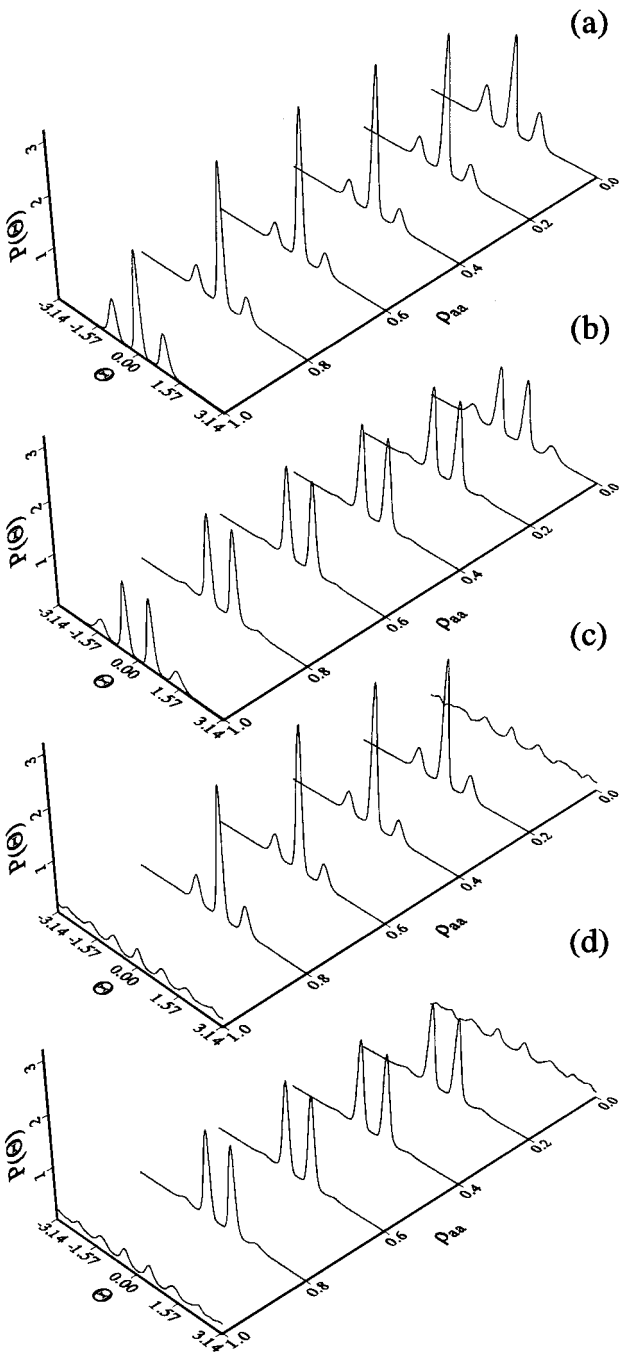

FIG. 10. Plots of the phase distribution $P(\theta)$ as functions of ρ_{aa}, for an initially coherent state with $\bar{n}=25$ and for $g\tau=5$ and various N: (a) $N=2$, (b) $N=3$, (c) $N=50$, and (d) $N=51$.

oscillation obtained when the cavity is pumped by excited atoms, but now the shape of the phase distribution remains the same contrary to the randomization of the phase observed before. The two- and three-peak structure of the phase distribution suggests that the micromaser field can be in a superposition of two or three states with well separated phase peaks. In Fig. 11 we plot the purity parameter for the case when initially the cavity field was in a coherent state with the mean number of photons $\bar{n}=25$ and atoms were strongly polarized $\rho_{aa}=\rho_{ab}=0.5$. The purity parameter shows some interesting features: after some oscillations as $g\tau$ increases, it

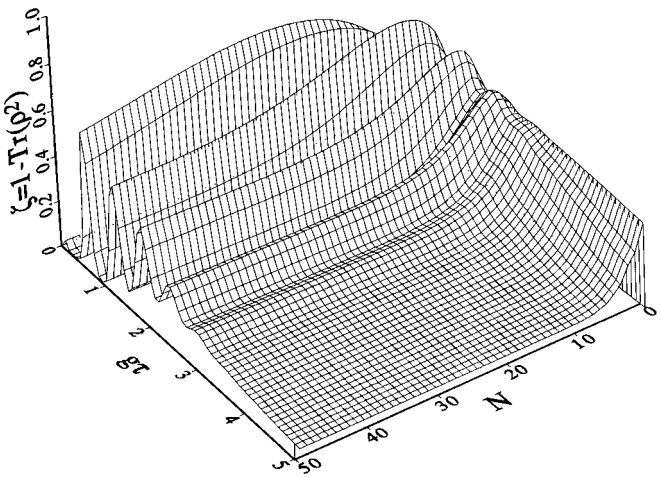

FIG. 11. Plot of the purity parameter as a function of N and $g\tau$ for an initially coherent state with $\bar{n}=25$ and for $\rho_{aa}=\rho_{ab}=0.5$.

becomes flat with sufficiently small values, which mean that for large values of $g\tau$ the cavity field evolves close to a pure state. There are no indications of the odd-even oscillations observed for the phase distribution. This suggests that these oscillations are associated with the phase only. To take a closer look at the effect we plot in Fig. 12 the matrix elements $\rho(n,m)$ of the field density matrix for (a) $N=2$ and (b) $N=3$. From Fig. 12 it is clear that for the odd number of atoms N some of the matrix elements become negative leading to a different state than that for an even number of atoms. This effect of switching between the two field states by every single atom passing the cavity appears to us to be very interesting, and the phase distribution studied in this paper proves to be a good means of discrimination between such states.

V. CONCLUSION

We have discussed the quantum phase properties of the field generated in the ideal micromaser cavity. The Pegg-Barnett phase formalism has been applied to find the phase probability distribution as well as the variance of the phase operator for the micromaser field. The recursion relation for the field density matrix is derived and used to get the evolution of the micromaser field. The phase probability distribution for the micromaser field shows some interesting features.

If the cavity field starts from a coherent state and atoms enter the cavity in their excited state, the phase distribution after N atoms passes through the cavity becomes an $(N+1)$-peak structure. For the large mean number of photons of the initial coherent state it is possible to obtain analytical expressions describing this structure and showing that the phase distribution is a weighted sum of the $N+1$ phase distributions for coherent states. When the number of atoms that passes through the cavity increases, the phase distribution becomes more and more flat, that is, the phase becomes more and more random, but the route to the completely random phase goes through an increasing number of peaks in the phase distribution.

On the other extreme, we have studied the phase proper-

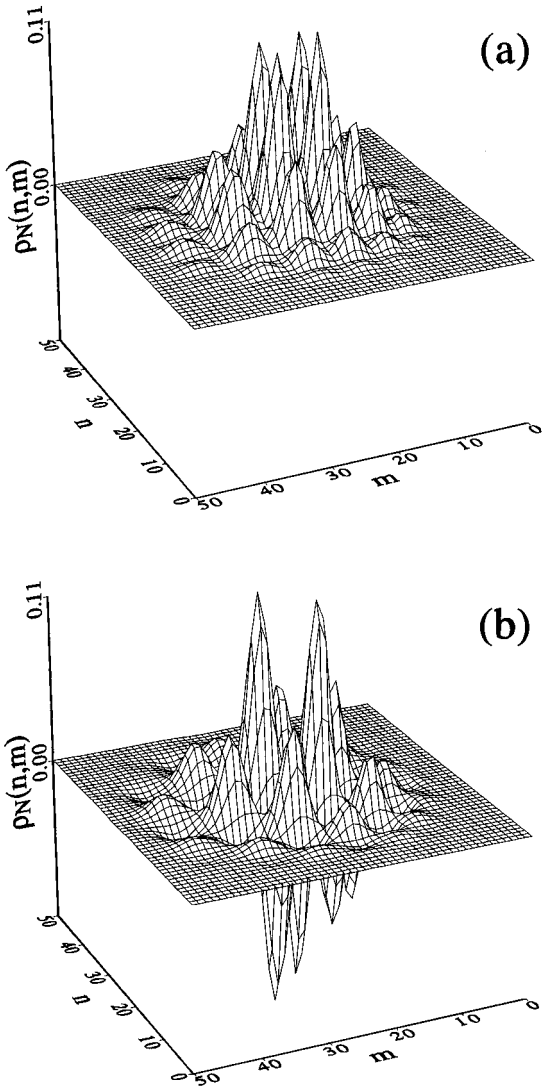

FIG. 12. Plots of the density-matrix elements $\rho_N(n,m)$ for $g\tau=5$ and the number of injected atoms (a) $N=2$ and (b) $N=3$. The cavity field is initially in a coherent state with $\bar{n}=25$ and is driven by polarized atoms with $\rho_{aa}=\rho_{ab}=0.5$.

ties of the cavity field for the cavity which initially was in the thermal state and is driven by highly polarized atoms. In this case the atomic phase is transferred to the field, and the cavity field can evolve to a state with a considerably well defined phase. We have shown that the phase transfer depends crucially on the atom-field interaction time. The state of the field can, as the number of interacting atoms increases, approach asymptotically a pure state which is identified as a 1-cotangent state if the interaction time is properly chosen. For a different choice of the interaction time the state of the field can be a mixed state with large phase as well as number fluctuations. We have numerically calculated and graphically presented results describing phase properties of the micromaser field for various initial conditions.

When the micromaser field is initially prepared in a coherent state and the cavity is pumped with polarized atoms interacting with the field for a particular time, the phase distribution of the cavity field that initially showed one phase peak starts to switch between two- and three-peak phase structures by every single atom that passes the cavity. The new phase structures do not depend on the number of atoms, but on whether an odd or even number of atoms have passed the cavity. This is a very interesting behavior of the micromaser field.

Our results were obtained under very strong assumptions: (i) a very high Q cavity that allows us to neglect the cavity damping, and (ii) well controllable atomic injections allowing for controlling both the velocity of the atoms as well as the time between the subsequent injections. This means that the model considered here is rather idealistic and it can be difficult to realize in practice. Nevertheless, we believe that the results reveal some interesting features of the micromaser.

In a more realistic model the cavity damping should be taken into account and it would necessarily lead to the broadening of the phase distribution due to the phase diffusion [9–12] associated with the nonzero cavity damping. The phase randomization discussed here has a quite different character and it is associated with the quantum properties of the field (granularity of the field) rather than with any damping processes. Even if the evolution is unitary, the field state can become a superposition of coherent states with the phase distribution exhibiting many peaks and thus being much broader than the distribution for a single coherent state. In this paper we have discussed the evolution of the micromaser phase properties of this dynamical character only, and it would be interesting to include the dissipation in the model.

ACKNOWLEDGMENTS

One of us (Ts. G.) would like to thank Professor H. Walther for the hospitality extended to him at the Max-Planck-Institut für Quantenoptik and acknowledge the Alexander von Humboldt Foundation for financial support. R. T. thanks the Polish Committee for Scientific Research (KBN) for financial support under Grant No. 2 P03B 128 8.

[1] The first masing using a single atom ''micromaser'' was reported by D. Meschede, H. Walther, and G. Müller, Phys. Rev. Lett. **54**, 551 (1985). For a review of the work of Walther and co-workers, see J. A. C. Gallas, G. Leuchs, H. Walther, and H. Figger, Adv. At. Mol. Phys. **20**, 413 (1985) and G. Raithel, C. Wagner, H. Walther, L. M. Narducci, and M. O. Scully, in *Cavity Quantum Electrodynamics*, edited by P. R. Berman (Academic, New York, 1994), p. 57.

[2] For a review of the work of S. Haroche and co-workers, see S. Haroche and J. M. Raimond, Adv. At. Mol. Phys. **20**, 350 (1985), and for the first realization of a two-photon micromaser, see M. Brune, J. M. Raimond, P. Goy, L. Davidovich, and S. Haroche, Phys. Rev. Lett. **59**, 1899 (1987).

[3] P. Filipowicz, J. Javanainen, and P. Meystre, Phys. Rev. A **34**,

3077 (1986); Opt. Commun. **58**, 327 (1986); J. Opt. Soc. Am. B **3**, 906 (1986).

[4] L. A. Lugiato, M. O. Scully, and H. Walther, Phys. Rev. A **36**, 740 (1987).

[5] E. T. Jaynes and F. W. Cummings, Proc. IEEE **51**, 59 (1963); N. B. Narozhny, J. J. Sanchez-Mondragon, and J. H. Eberly, Phys. Rev. A **23**, 236 (1981); G. Rempe, H. Walther, and N. Klein, Phys. Rev. Lett. **58**, 353 (1987).

[6] J. Krause, M. O. Scully, and H. Walther, Phys. Rev. A **36**, 4547 (1987).

[7] P. Meystre, G. Rempe, and H. Walther, Opt. Lett. **13**, 1078 (1988).

[8] J. Krause, M. O. Scully, and H. Walther, Phys. Rev. A **34**, 2032 (1986).

[9] M. O. Scully, H. Walther, G. S. Agarwal, Tran Quang, and W. Schleich, Phys. Rev. A **44**, 5992 (1991).

[10] R. J. Brecha, A. Peters, C. Wagner, and H. Walther, Phys. Rev. A **46**, 567 (1992).

[11] C. Wagner, R. J. Brecha, A. Schenzle, and H. Walther, Phys. Rev. A **47**, 5068 (1993).

[12] W. C. Schieve and R. R. McGowan, Phys. Rev. A **48**, 2315 (1993).

[13] Fam Le Kien, M. O. Scully, and H. Walther, Found. Phys. **23**, 177 (1993).

[14] J. J. Slosser, P. Meystre, and S. Braunstein, Phys. Rev. Lett. **63**, 934 (1989); J. J. Slosser and P. Meystre, Phys. Rev. A **41**, 3867 (1990).

[15] P. Meystre, J. J. Slosser, and M. Wilkens, Phys. Rev. A **43**, 4959 (1991).

[16] Fam Le Kien, Phys. Rev. A **44**, 3282 (1991).

[17] D. T. Pegg and S. M. Barnett, Phys. Rev. A **39**, 1665 (1989); S. M. Barnett and D. T. Pegg, J. Mod. Opt. **36**, 7 (1989).

[18] S. Stenholm, Phys. Rep. C **6**, 1 (1973).

[19] H. T. Dung, R. Tanaś, and A. S. Shumovsky, Opt. Commun. **79**, 462 (1990).

[20] G. Drobný, Ts. Gantsog, and I. Jex, Phys. Rev. A **49**, 622 (1994).